INTERNAL CHARGING IN SPACE

D J Rodgers and K A Ryden
Space Department, Defence Evaluation & Research Agency, Farnborough, Hampshire, GU14 0LX, UK
djrodgers@scs.dera.gov.uk

ABSTRACT

Internal charging results in high electric fields within spacecraft dielectric materials. This poses a hazard to electronic systems from electrostatic discharges (ESDs). Many spacecraft anomalies are believed to have been caused by this process. Hazardous internal charging environments are found in the outer electron radiation belt, during strong enhancements. Because of the dynamic nature of the charging process, mean radiation belt models are not appropriate for assessing the risk from this process and suitable 'worst-case' environment models must be used. Calculations of internal fields require both the simulation of the current deposited in the material and the ability of the material to leak away current through conduction. Monte Carlo codes can be used for the current deposition problem and there are a number of 1-d codes that also simulate conducted currents, for simple geometries. Where a potential risk has been identified, designers can employ a number of mitigation procedures to lessen the risk of discharges.

ESDs are not the only hazard from internal charging. Some electric field sensitive systems may be degraded by internal charging effects.

1. INTRODUCTION

Internal charging refers to the build-up of electric charge, due to particles from the external space environment, anywhere within the spacecraft structure except on its surface. In many cases, this occurs inside dielectrics and is often called deep-dielectric charging. However, internal charging may also occur on electrically isolated conductors within the spacecraft.

The distinction between surface and deep-dielectric charging may, on occasions, be fuzzy since thick dielectrics on the spacecraft surface are subject to charge deposition over a range of depths and charge build-up near the surface and deeper within the material both contribute to the total strength of electric fields within the structure. However, there are practical reasons for treating internal and surface charging separately:

- Surface charging is associated with large currents of a low-energy (~10 keV) plasma population which typically varies on time-scales of minutes. Secondary and photo-emission are major considerations and are often the dominant currents. The time-scale for charging to occur is typically seconds for absolute charging and minutes for differential charging. These time-scales are associated with the time taken for equilibrium between primary and secondary currents to be achieved and the inter-surface capacitative time-constant. These time scales are too short for significant charge to pass through the insulator by internal conduction.
- Internal charging is associated with small currents of a higher-energy (typically >0.5MeV) electron population which typically varies on time scales of hours to days. Photo-emission is not a consideration because the region of interest is not exposed to sunlight. Secondary emission is generally unimportant since secondary emission yields are low at the primary energies concerned. The time scale for charging is often days or longer and is typically determined by the capacitative time-constant across the material. Internally conducted current is a significant contributor to the overall current balance.

Surface deposited current does, in principle, contribute to the currents flowing within dielectrics and hence to the internal charge state. However, in practice, on the long time-scales associated with hazardous levels of internal charging, surface deposited current tends to be neutralised by the other surface currents and hence appears only as an effectively grounded surface, from the point of view of internal charging.

2. WHY IS INTERNAL CHARGING A PROBLEM?

Internal charging becomes a problem when the stored charge undergoes a sudden discharge or dielectric breakdown. The most immediate effect is the direct injection of large transient currents into electronic circuits or the indirect production of transient currents through electromagnetic coupling. Additionally, breakdown may cause a permanent change in the material properties which may cause the material to be degraded as an insulator. It is sometimes observed that, once an internal charging anomaly has first occurred, it is able to recur more frequently in less extreme environments. A typical internal charging anomaly was observed on the DRA-δ spacecraft [1] and is illustrated in figure 1 below. The anomaly occurred almost every time that daily >2MeV electron fluence exceeded a threshold of 5×10^7 $cm^{-2}day^{-1}sr^{-1}$.

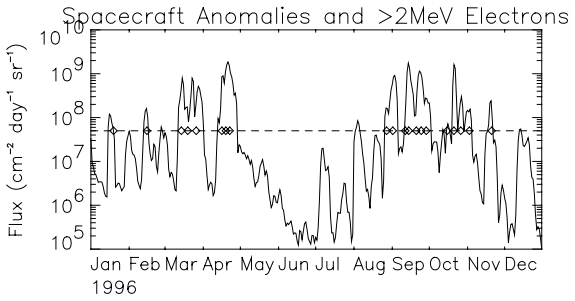

Figure 1 Times of occurrence of a certain anomaly on DRA-δ (◊), compared to >2MeV electron flux from GOES. [*data courtesy of NOAA/SEC*]

Electric breakdown requires high electric fields and is thought to be caused by avalanche effects i.e. an energetic carrier attains sufficient energy between collisions with static molecules to give a high probability of ionisation in order to generate more carriers, which leads to current multiplication. These discharges characteristically produce a 'tree'-shaped discharge path called a Lichtenberg pattern.

Published breakdown electric fields for dielectrics are typically close to 10^7V/m however, in laboratory experiments [2] pulsing has often been seen at lower field strengths and so a value of 10^6V/m is a reasonable 'danger-level', that should be avoided.

3. EQUILIBRIUM ELECTRIC FIELD

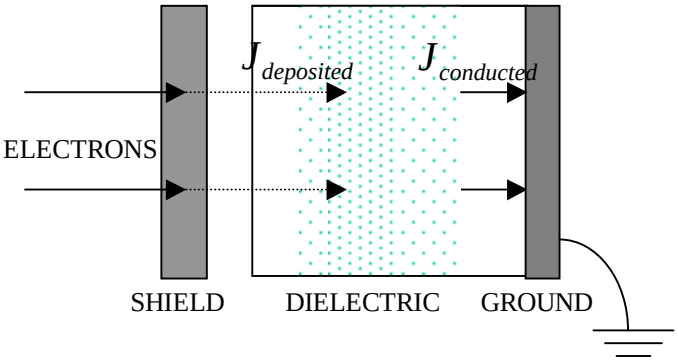

Figure 2 1-d schematic diagram of the internal charging process.

As is shown schematically in figure 2, electrons from the external environment are usually substantially attenuated by spacecraft shielding, if present, before a portion is stopped within the dielectric to produce a current of deposited charge, $J_{deposited.}$ This gradually builds up an electric field between the area of deposition and the ground plane. This field drives a conducted current, $J_{conducted}$, which can be calculated from Ohm's Law, i.e.

$$E = J_{conducted} / \sigma$$

Here E is the electric field and σ is the bulk conductivity. The conducted current is initially small but eventually an equilibrium is established in which the conducted current equals the deposited current. This equilibrium electric field is the maximum i.e. worst-case achievable by the structure in that environment. The magnitude of the equilibrium field depends on both the amount of deposited current and on the conductivity throughout the material.

4. CHARGE DEPOSITION

Radiation belt electrons penetrate spacecraft surfaces and are deposited within internal materials. Their penetration depth is dependent on their energy and the material properties, particularly its density. This may be calculated to good accuracy using Monte Carlo particle transport codes such as ITS [3] or GEANT [4]. There also a number of empirically derived formulae relating range, R (=penetration depth x material density) to incident electron energy, e.g. Feather (1921) [5], Glendenin & Coryell (1948) [6], Katz and Penfold (1952) [7] and Weber (1964) [8]. Comparisons of these formulae [6] showed that they give very similar results apart from the particularly simple Feather formula which diverges from the others below about 400keV. The formula of Weber [8] is shown below:

$$R = 0.55.E.\left[1 - \frac{0.9841}{(1+3E)}\right] \quad \text{g cm}^{-2}$$

Here E is energy in MeV. Excellent agreement between this formula and Monte Carlo simulations using the ITS and GEANT codes has been reported [9].

Whilst R determines the maximum penetration depth of electrons, they are deposited almost uniformly over a distance a [10] where:

$$a = 0.283.E \quad \text{g cm}^{-2}$$

This is illustrated in figure 3.

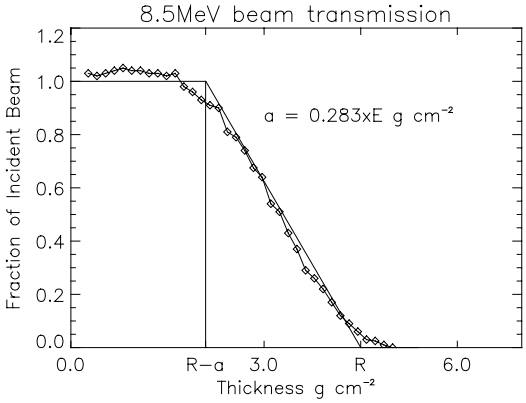

Figure 3 Diamonds show an ITS simulation of the penetration of a mono-energetic electron beam in Aluminium.

5. CONDUCTIVITY

On dielectric materials, only a small number of electron-hole pairs are available to carry charge. These are created when thermal excitation pushes an electron into the conduction band. These electrons become trapped in trapping sites that are potential wells within the material, as is shown in figure 4A. Higher temperatures increase the energy available to trapped electrons, allowing more of them to jump from one trapping site to another. Hence conductivity increases with temperature – the reverse of the dependence observed in conductors.

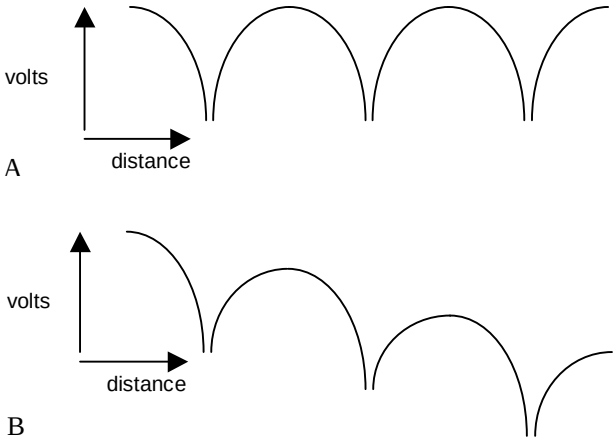

Figure 4 A - Schematic diagram of potential well structure , B – with an imposed electric field.

The dependence of conductivity on temperature T is generally represented by the following equation:

$$\sigma(T) = \sigma_{\infty} \exp\left(-\frac{E_A}{kT}\right)$$

where E_A is the material dependent activation energy, k is Boltzman's constant and σ_{∞} is the maximum conductivity as T approaches infinity.

It is important to note that E_A is not the band-gap associated with the excitation of electrons from the valance band into the conduction band which is far larger (for polythene E_A is around 1 eV and the band gap is around 8.8 eV). Clearly a more subtle process is at work than a straightforward excitation of electrons. E_A is found from experimental studies and typically lies in the region of 1eV for most dielectrics. Some values were calculated [11] and are listed below.

Material	E_A
PMMA (perspex, plexiglas)	1.7 eV
Polythene	1.0 eV
Glass (typical)	1.3 eV

Based on the its activation energy, the strong temperature dependence of conductivity in Polythene is shown in figure 5. Changing from 25°C to 0°C would lower conductivity by a factor of 30.

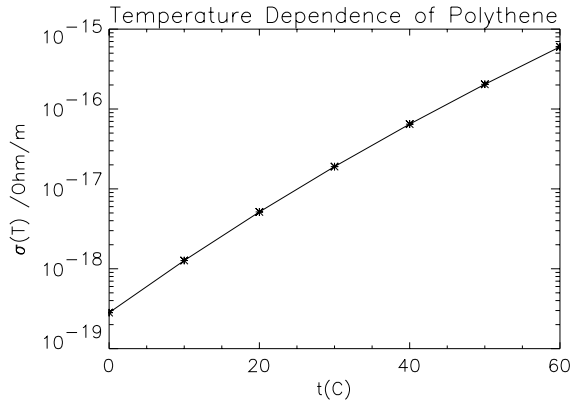

Figure 5 Temperature dependence of Polythene

Field enhanced conductivity is attributed to the strong electric field causing the activation of additional carriers as well as increasing the mobility of carriers by reducing the potential barriers between trapping sites, as shown in figure 4B. The most up-to-date treatment appears to be that of Adamec and Calderwood (A&C) [12] in 1975. Even so, their model was not significantly different from earlier work carried out in the 1930s, since A&C showed that their model yielded almost identical results to that of Onsager (1934) [13]. The A&C relation between electric field and conductivity is:

$$\sigma(E,T) = \sigma(T)\left(\frac{2+\cosh(\beta_F E^{1/2}/2kT)}{3}\right)\left(\frac{2kT}{eE\delta}\sinh\left(\frac{eE\delta}{2kT}\right)\right)$$

where E is electric field, $\beta_F = \sqrt{\frac{e^3}{\pi\varepsilon}}$, δ is jump distance (fixed at 10 angstroms), e is the charge on an electron, ε is permittivity. This formula is essentially theoretical, except that δ was chosen to fit experimental data.

Figure 6 shows the change in conductivity due to electric field. Up until the 10^6V/m there is virtually no effect. Since dielectrics at this field level already have a substantial disk of ESD, it appears that electric field induced conductivity has little effect on whether dangerous levels of charging occur.

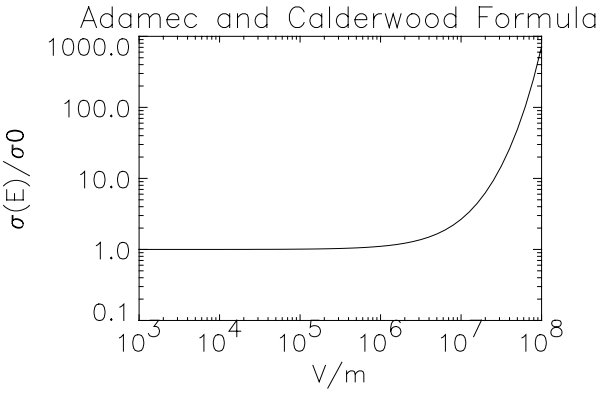

Figure 6 Electric field dependence for a typical polymer according to the Adamec & Calderwood formula.

Polymers demonstrate an increase in conductivity under irradiation and this effect has been subject to much experimental investigation, although most was conducted at very high dose rates by comparison with that seen in space applications. Irradiation excites electrons into the conduction band, generating charge carriers in proportion to the energy absorption rate in the polymer i.e. dose rate. This dose rate may be the result of energetic electrons, ions or gamma rays.

The basic equation to describe the conductivity, of irradiated polymers was developed by Fowler (1956) [14]. This equation, shown below, is widely used:

$$\sigma = \sigma_o + k_p \dot{D}^{\Delta} \quad \Omega^{-1}\,\mathrm{cm}^{-1}$$

where σ_o is the dark conductivity, k_p is the material-dependant co-efficient of prompt radiation induced conductivity and Δ is a dimensionless material-dependent exponent ($\Delta<1$). An example of the effect of dose rate on conductivity is given in figure 7 for FEP-Teflon. This fits well with the Fowler formula.

It is generally observed that after irradiation is stopped, radiation-induced conductivity decays away only slowly [15] as is shown, for Kapton, in figure 8. This slow decay is often called 'delayed' radiation-induced conductivity. In some cases a linear dose-dependent permanent increase in conductivity is also thought to occur. However, this phenomenon seems to be much less well reported and may be restricted to certain polymers which are prone to undergoing permanent changes under irradiation.

Unlike polymers, electrical conductivity in glasses is ionic i.e. current is carried by the migration of ions as in electrolytes rather than by electron-hole pairs. The sodium ion with a relatively high mobility is responsible for the greater part of the conductivity. Irradiation does not seem to be reported to increase conductivity, presumably because it has no effect on the concentration of the sodium ions.

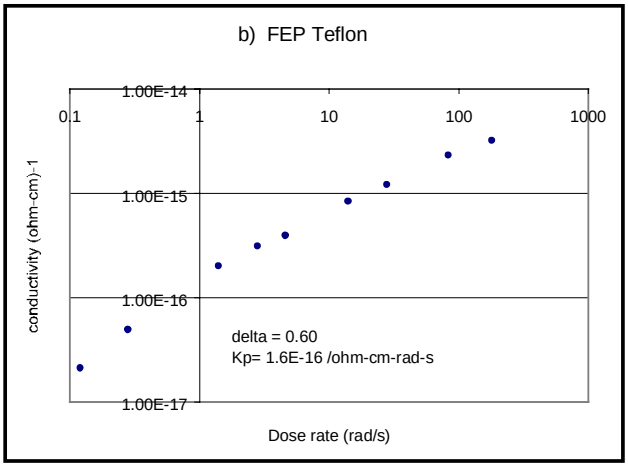

Figure 7 Dependence of conductivity on dose rate for FEP Teflon. [11]

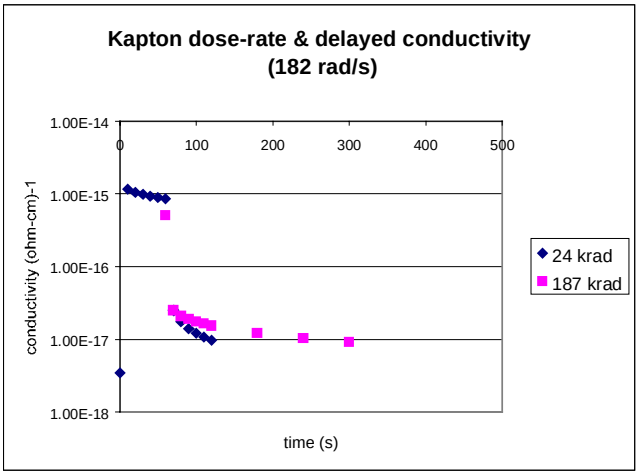

Figure 8 Delayed radiation-induced conductivity observed in Kapton [11].

Because of the crucial role played by conductivity in the overall assessment of the internal charging threat, it is important that it is the bulk conductivity that is used in charging calculations. Conductivity measurements may be dominated by time-dependent polarisation effects lasting hours or longer. Hence investigators should be cautious about using conductivity values quoted in materials literature, since is standard practice [16,17] for these to be measured after only 60s.

6. CHARGING TIME SCALE

When the electron environment is enhanced, the response of the dielectric is not instantaneous. For a planar dielectric, the electric field approaches the equilibrium electric field exponentially with time t, i.e.

$$E = \frac{J}{\sigma}\left(1 - \exp\frac{-t}{\tau}\right)$$

where τ is a time constant. This is the same formula as for a planar capacitor. Where the electrical properties of the dielectric are constant across the material $\tau = \varepsilon/\sigma$ where ε is the permittivity.

It can be easily shown that the equilibrium electric field is proportional to τ and so only materials with long time constants are susceptible to hazardous levels of internal charging. Typically a time constant of 1 day or longer is associated with susceptible materials. τ is effectively the period over which electron fluxes are integrated by the material. Hence 1-day time averages of electron flux give appropriate temporal resolution for defining a hazardous internal charging environment.

7. THE CHARGING ENVIRONMENT

Electrons responsible for internal charging are found in both the inner and outer radiation belts. The intensity of the outer belt reaches the highest levels, particularly at higher energies. In practice, high levels of radiation protection against protons and high dose rates probably prevent serious charging in most spacecraft in the inner belt so that only the outer belt is associated with internal charging anomalies. Although satellites in geostationary orbit are far from the peak of the outer belt, they are subject to continuous exposure and experience a significant risk of internal charging effects. The outer belt is highly dynamic and >2MeV electron fluxes can rise by 2 or 3 orders of magnitude over a period of hours. Such enhancements may persist for several days. Figure 9 illustrates the way outer belt fluxes rise and fall. The data come from the cold ion detector on STRV-1a, which was sensitive to electrons with energies greater than about 1MeV.

Outer belt fluxes depend strongly on L-shell and solar cycle phase. Peak fluxes are typically an order of magnitude higher during the declining phase of the solar cycle than at solar maximum.

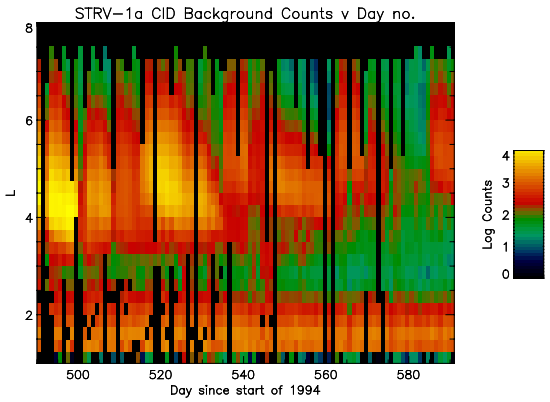

Figure 9 Background counts in the STRV-1a CID instrument as a function of L-shell and time.

Average models of the radiation belts, like AE-8, which are commonly used for dose predictions, are inadequate for assessing susceptibility to internal charging levels. Instead 'worst-case' environments need to be used. Strictly, different structures may have different worst-case environments. For instance, a surface component is most sensitive to soft spectra while a well-shielded component is more sensitive to hard spectra. However, flux enhancements are usually associated with spectral hardening [18] and so a general worst-case model can be created. One such model, called FLUMIC [18] has been created for the whole outer belt in a DERA-led study. For geostationary orbit, the same study defined a worst-case environment of the following form:

$$Flux(E) = F_R \exp\frac{(2-E)}{E_0}$$ where E_0=0.63 MeV and F_R=6x10^9 cm^{-2}day^{-1}sr^{-1}

A NASA worst-case environment has also been defined [19]. These two GEO worst-case spectra are compared in figure 10. The NASA model is more severe at low energies. This difference probably stems from the different averaging periods used for the models (several hours for NASA, longer than 1day for DERA).

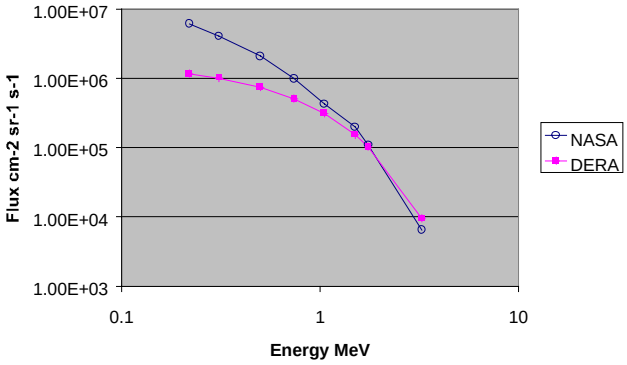

Figure 10 Comparison of NASA and DERA geostationary worst-case environments.

8. GEOMETRIC CONSIDERATIONS

Internal charging can be most easily calculated by considering a 1-d planar structure. However, even in this simple case, the conductivity will vary across the material due to the changing electric field and radiation induced conductivities. The electric field will vary across the dielectric and maximum electric field is to be found at the boundary between the dielectric and the underlying conductor.

Cable insulators usually exhibit 1-d cylindrical symmetry. For a cable with a single central conductor, the cylindrical shape leads to a concentration of current as it flows to the centre. This increases the electric field over the equivalent planar case.

For insulators with a complicated 3-d structure, calculation of the maximum electric field requires both a 3-d model of the charge deposition and a 3-d model of the currents and electric fields. However, even in this case, the maximum electric field is expected to occur at a dielectric/conductor boundary.

Conductors cannot support internal electric fields. However, isolated conductors usually have a dielectric between them and a grounded surface. In just the same way as for a dielectric alone, the electric field across the dielectric will rise until the conducted current equals the combined current deposited in the conductor and dielectric.

9. HAZARD ASSESSMENT

To assess the vulnerability of a structure to internal charging, one can compare its behaviour to a well studied system, such as the CRRES IDM [20]. This system saw occasional pulses when fluxes in a 10 hour period exceeded $2x10^9$ cm^{-2}. Shielding to avoid fluxes exceeding this level should prevent ESDs in similar systems but may lead to over-protection or under-protection if the system is substantially different.

A more quantitative approach is to use a simulation tool such as DICTAT [21] or ESADDC [22] to estimate the maximum electric field. The former is a 1-d analytical code and is available in ESA's SPENVIS system [23]. The latter is a 1-d Monte Carlo code. Both codes take into account changes in material conductivity and require good material characterisation as input. There is also an internal charging module in the SEE NASA Interactive Charging Handbook [24] currently available only within the USA. In addition, several institutions have their own internal software.

10. MITIGATION

Where an ESD risk has been identified, there are a number of steps that may be taken, perhaps together, to minimize the risk of anomalies:

- Control of environment
  - avoiding hazardous regions
- Control of deposited current
  - thick shields
  - thin dielectrics
- Control of dielectric conductivity
  - leaky insulators
  - high temperatures
- Control of circuit sensitivity
  - slow electronic circuits
  - pulse filtering and damping resistors
- Control of software sensitivity
  - error detection and correction

11. ELECTRIC FIELD SENSITIVE SYSTEMS

ESD-induced anomalies are not the only hazard from internal charging. It may also affect systems where electric fields need to be measured or controlled accurately but where components are insulators, semiconductors or electrically isolated conductors.

Tri-axial accelerometers represent a uniquely sensitive case of an isolated conductor. In these instruments acceleration e.g. due to drag or gravity gradient, is measured by the force required to maintain a metallic test mass stationary in 3 dimensions between electrodes e.g. as implemented in the ASTRE accelerometer [25]. Alternatively, the test mass may be floating freely, with the spacecraft keeping station around it, as in the forthcoming LISA gravitational astronomy mission [26]. Any electrical charging of the mass, due to deposition of penetrating particles will produce an additional electrostatic force that is indistinguishable from the acceleration being measured. Some accelerometers have used a fine wire for grounding but this can compromise accuracy. Alternatively, controlled discharging by photo-emission, using a UV source, may be conducted. To minimise internal charging, such an instrument needs to be shielded from penetrating particles. It is an unusual feature of such systems that it is penetrating ions (>100MeV) that represent the greatest hazard. Past missions have experienced enhanced charging in LEO when passing through the South Atlantic Anomaly [25] while missions in GEO or interplanetary space may be subject to Solar energetic particle events.

In a similar way, accelerometers built as micro-electromechanical systems (MEMS) can be affected by radiation-induced electric fields. These systems have electronic and mechanical parts integrated on the same semiconducting chip. These can include thin insulating layers of e.g. SiO_2 or Si_3N_4. Dose-dependent

production of electron-hole pairs can lead to charge trapping in the insulator. In one study [27] a certain 1-d MEMS accelerometer was shown to exhibit spurious measurements under proton irradiation of its mechanical part. A similar device, in which the dielectric layer was electrically shielded by a conductor did not experience the same problem.

12. CONCLUSIONS

Despite our long experience with spacecraft ESD effects, internal charging is proving to be a persistent source of spacecraft anomalies. Dielectric materials are found throughout a spacecraft, often in cold locations and it is virtually impossible to give them all adequate shielding. Trends in spacecraft technology are leading to more ESD-sensitive devices and lighter, less shielded structures. Hence internal charging needs to be considered in modern spacecraft design and is likely to continue to pose problems in the future

ACKNOWLEDGEMENTS

Many of the insights into internal charging described here were obtained while working in collaboration with John Sorensen (ESA), Leon Levy (ONERA), Gordon Wrenn (T.S. Space Systems) and Paul Latham (DERA). Paul Morris (DERA) is thanked for his conductivity measurements.

REFERENCES

[1] Wrenn G.L., Conclusive evidence for internal dielectric charging anomalies on geosynchronous communications spacecraft, *J.Spacecraft& Rockets,* vol.32, no.3, pp.514-520, 1995

[2] D.J.Rodgers, K.A.Ryden, P.M.Latham, L.Lévy and G.Panabière, 1999 Engineering Tools for Internal Charging, Final Report on ESA contract no. 12115/96/NL/JG(SC), DERA/CIS(CIS2)/7/36/2/ 4/FINAL, 1999 (www.estec.esa.nl/wmwww/ WMA/reports/idc/final_report.pdf)

[3] Halbleib J.A. et al. ITS version 3.0: The Integrated TIGER Series of Coupled Electron/Photon Monte Carlo Transport Codes, Sandia National Laboratories, Mar 1992

[4] Brun R. et al. GEANT User's Guide 1993

[5] Chadwick, J., Radioactivity and radioactive substances, Pitman, London, 1921.

[6] Glendenin and Coryell, *Nucleonics*, 1, 31, 1948.

[7] Katz, I. and A.S. Penfold, *Rev. Mod. Phys*., 24, 28, 1952.

[8] Weber, K.H., *Nucl. Inst. Meth*., 25, pp. 261, 1964.

[9] Trenkel, C., Comparison of GEANT 3.15 and ITS 3.0 Radiation Transport Codes, ESA working paper, EWP 1747, 1993.

[10] Sørensen J., An engineering specification of internal charging, p.129 Environment Modelling for Space-based Applications ESA SP-392, 1996

[11] D.J.Rodgers, K.A.Ryden, P.M.Latham, G.L.Wrenn, L.Lévy, and B.Dirassen, Engineering Tools for Internal Charging, Final Report on ESA contract no. 12115/96/NL/JG(SC) CCN no.2, DERA/CIS/CIS2/CR000277, 2000

[12] Adamec, V. and J. Calderwood, *J Phys. D: Appl. Phys.*, 8, 551-560, 1975.

[13] Onsager, L., *J Chem. Phys.*, 2, 599-615, 1934..

[14] Fowler, J.F., *Proc. Royal Soc., London, A* 236, 464, 1956.

[15] Weaver L., J.Shultis, and R.Faw, Analytic solutions for radiation induced conductivity in insulators, *J. Appl. Phys*., 48, No. 7, 1977.

[16] Methods of test for volume resistivity and surface resistivity of solid electrical insulating materials, IEC 93, Second Edition 1980.

[17] Standard test methods for DC resistance or conductance of insulating materials, ASTM D 257-93 (1993, Re-approved 1998).

[18] Wrenn G.L., D.J.Rodgers and P.Buehler Modelling the Outer Belt Enhancements of MeV Electrons, *J.Spacecraft & Rockets,* vol.37, no.3, pp.408-415, 2000

[19] Avoiding Problems caused by Spacecraft On-orbit Internal Charging Effects, NASA Technical Handbook, NASA-HDBK-4002, February 17, 1999

[20] Frederickson, A. R., Holeman, E. G., and Mullen, E. G., Characteristics of Spontaneous Electrical Discharging of Various Insulators in Space Radiations, *IEEE Trans. Nucl. Sci*., Vol. 39, No. 6, pp. 1773-1982, 1992

[21] An Engineering Tool for the Prediction of Internal Dielectric Charging,D.J.Rodgers, K.A.Ryden, G.L.Wrenn, P.M.Latham and J.Sorensen, 'Proceedings 6th Spacecraft Charging technology Conference', Hansom AFB, 1998

[22] Soubeyran, A. and Floberhagen R., 'ESA-DDC 1.1 User Manual', Matra-Marconi Space, 1994.

[23] www.spenvis.oma.be/spenvis/

[24] Katz I., V.Davis, M.Mandell, B.Gardner, J.Hilton, A.Fredrickson, D.Cooke and J.Minor, Spacecraft Charging Interactive Handbook, this volume, 2001

[25] Touboul P., B.Foulon and E.Willemenot, Electrostatic space accelerometers for present and future missions, *Acta Astronautica*, 45, no.10, pp.605-617, 1999

[26] LISA Pre-Phase A Report, Second Edition, July 1998 http://lisa.jpl.nasa.gov/documents/ppa2-09.pdf

[27] Knudson A.R., S.Buchner, P.McDonald, W.J.Stapor, S.Lewis and Y.Zhao, The effects of radiation on MEMS accelerometers, *IEEE Trans. Nucl. Sci*, 43, no.6, pp.3122-3126, 1996